Bistable Electro-optical Fast Switching for Induced Smectic (Liquid Crystalline Polymer/Liquid Crystals) and (Pseudo Liquid Crystalline Copolymer/Liquid Crystals) Composite Systems

Hirokazu Yamane, Hirotsugu Kikuchi, and Tisato Kajiyama*

Department of Chemical Science and Technology, Faculty of Engineering, Kyushu University, 6-10-1 Hakozaki, Higashi-ku, Fukuoka 812-81, Japan

Received December 3, 1996; Revised Manuscript Received April 1, 1997[⊗]

ABSTRACT: Reversible and bistable electro-optical switching characteristics of induced smectic composite systems composed of a side chain nematic liquid crystalline polymer (nematic LCP) and its copolymer with weak polar methoxy terminal groups in the side chains and low molecular weight nematic liquid crystals (nematic LCs) with each strong polar cyano end have been investigated. The liquid crystalline copolymer (LCcoP) with weak polar methoxy terminal groups in the side chains was used to improve the response speed at room temperature for the bistable and reversible light switching of the binary composite system. Since LCcoP with 52.5 mol % substituted mesogenic side chains did not exhibit mesophase characteristics, this LCcoP was named as pseudo LCcoP in the present study. The (pseudo LCcoP/nematic LCs) composite system showed an induced smectic phase over a wide range of mixing concentration and temperature. A reversible and bistable electro-optical switching with a short response time (∼100 ms) was realized for the induced smectic binary composite system upon the application of an appropriate electric field at room temperature. Also, the binary composite system showed a reversible and bistable electro-optical switching based on the sign reversal of the dielectric anisotropy upon the application of ac electric fields with high (∼kHz) and higher (∼100 kHz) driving frequencies.

Introduction

The structure and physical properties of side chain liquid crystalline polymers (LCPs) have been widely explored.[1] LCPs are new types of substances combining the properties of low molecular weight liquid crystals (LCs) such as variable optical anisotropy, induced orientation in an external electromagnetic field, high mobility, birefringence, dielectric properties, viscous flow, surface-induced orientation, etc. and also those of polymers such as elasticity, easy fabrication as solid films, etc. LCPs have a strong tendency to form a glassy state on cooling, which provides the possibility of freezing in and stabilizing the mesomorphic structure in solid polymer films. The application of LCPs in a glassy phase for optical data storage, that is, write-once and erasable thermo-optical recording, has been demonstrated since 1983.[2−5] All specific anisotropic properties of LCPs are quite similar to those of LCs. An exception is the much higher viscosity of LCPs, resulting in slower response with respect to external agencies like electric and magnetic fields and mechanical deformation.

In order to improve the switching speed of LCPs, the binary systems composed of a side chain LCP and an LC that has a chemical structure similar to that of the mesogenic side chain in the LCP were studied.[6−8] The (LCP/LC) composite systems showed faster switching speeds than LCP itself because of reducing the viscosity. Furthermore, the binary composite system in a homogeneous smectic phase exhibited reversible and bistable electro-optical switching upon the application of ac electric fields with two different frequencies. The smectic binary composite systems exhibited a highly transparent state upon the application of an ac electric field with a high frequency (∼kHz) and turned into a remarkable light scattering state upon the application of a field with a low frequency (∼Hz) or dc.[8−10] Each transparent and turbid state was stably memorized after the removal of electric fields due to the strength of smectic layers in the composite systems. The turbid and transparent states may occur from a balance between an electric current effect based on electrohydrodynamic motion of the LCP main chains and an electric field effect based on the dielectric anisotropy of the LC molecules and the side chain part of the LCP. However, this binary composite system could not be driven at room temperature and the response time was around several seconds upon $E = 8.84$ Vrms·μm^{-1} at 367 K.[9,10]

Various methods toward the optimum smectic binary composite system with a faster bistable switching speed and stable memory characteristics at room temperature have been tried by using different LCPs or liquid crystalline copolymers (LCcoPs).[11] It is well-known that the binary mixtures composed of nematic LCs with a strong polar cyano or nitro terminal group and a weak polar one induce a smectic phase.[12−15] This concept was applied to the binary mixture of nematic LCP with weak polar end groups in the side chains and nematic LC with a strong polar end group in order to reduce the response time for bistable and reversible light switching. The response speed for the (nematic LCP/nematic LC) composite system in an induced smectic state was several seconds at above room temperature.[16,17] Another method to prepare the optimum composite system with a rapid bistable switching speed has been demonstrated by using smectic LCcoP with dimethylsiloxane groups in the main chain. Since the main chain of a smectic LCcoP has a remarkably high mobility at room temperature, a smectic LCcoP/nematic LCs composite system in a smectic state might exhibit faster electro-optical switching with a bistable memory effect at room temperature.[18]

In this study, a novel type of pseudo LCcoP with a small fraction of substituted mesogenic side chains with weak polar terminal groups has been used to prepare

* To whom correspondence should be addressed.
[⊗] Abstract published in *Advance ACS Abstracts,* May 1, 1997.

S0024-9297(96)01754-8 CCC: $14.00

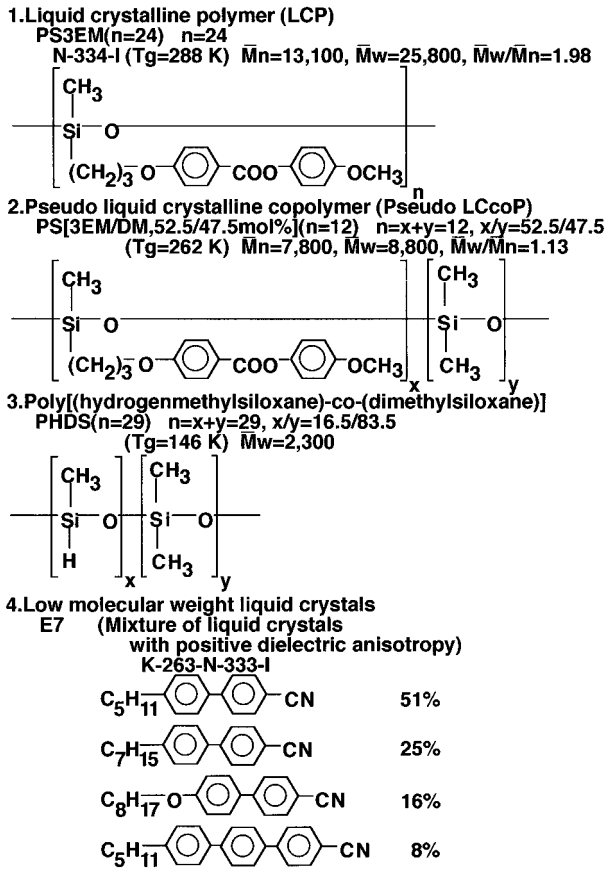

Figure 1. Chemical structures and physical properties of nematic liquid crystalline polymer with weak polar terminal groups (1), pseudo liquid crystalline copolymer with weak polar terminal groups (2), poly[(methylsiloxane)-*co*-(dimethylsiloxane)] (3), and low molecular weight nematic liquid crystals with each strong polar terminal group (4).

an induced smectic composite system with an improved response speed for bistable light switching at room temperature. Mesomorphic characteristics and electro-optical properties of the induced smectic (pseudo LCcoP/nematic LCs) composite system have been compared with those of the composite system composed of the corresponding nematic LCP.

Experimental Section

Figure 1 shows the chemical structures and physical properties of a nematic LCP, a pseudo LCcoP, a siloxane copolymer, and nematic LCs used in this study. The LCP and the pseudo LCcoP were poly[(((((4-methoxyphenoxy)carbonyl)-phenoxy)propyl)methylsiloxane] (PS3EM(n = 24)) and poly-[((((((4-methoxyphenoxy)carbonyl)phenoxy)propylmethylsiloxane)-*co*-(dimethylsiloxane)] (PS(3EM/DM)(n = 12)). PS3EM(n = 24) and pseudo PS(3EM/DM)(n = 12) were synthesized by a standard method reported by Finkelmann *et al.*[19] Their chemical structures were confirmed by NMR and FT-IR, and their average degrees of polymerization n, number and weight average molecular weights M_n and M_w, weight to number average molecular weight ratios M_w/M_n, and purities were determined by gel permeation chromatography in tetrahydrofuran using polystyrene standards. The siloxane copolymer was poly[(methylsiloxane)-*co*-(dimethylsiloxane), 16.5/83.5 mol %](n = 29) (PHDS(n = 29), Chisso Co. Ltd. PS123.5). Also, nematic LCs were commercial liquid crystals of E7, a eutectic nematic mixture. E7 shows a positive dielectric anisotropy. The binary composite systems were prepared from an acetone solution of (LCP/LCs) and (LCcoP/LCs) by a solvent casting method. The phase transition behavior and the aggregation states of the binary composites were investigated on the basis of differential scanning calorimetry (DSC), polarizing optical microscopy (POM), and X-ray diffraction (WAXD) studies, in order to determine the phase diagrams of the binary composite systems. Also, in order to evaluate the molecular mobility of LCP and pseudo LCcoP, the dielectric relaxation processes were observed as a function of temperature and frequency using an impedance analyzer (YHP 4192A LF). The dielectric relaxation measurements of siloxane polymers were carried out in the frequency range from 100 Hz to 10 MHz and the temperature range from 183 to 403 K in order to compare the molecular mobilities of the main chains. The experimental setup used for the measurement of the electro-optical switching characteristics is illustrated in Figure 2. The composite film was sandwiched between two indium−tin oxide (ITO)-coated glass plates (dimensions 5 mm × 5 mm) which were separated by the PET film spacer of 10 μm thick. All samples were measured in an unaligned state. The temperature of the sample was computer-controlled by a custom made nichrome heating system using a thermocontroller with a resolution of ±0.04 K. A He−Ne laser providing 2 mW at 632.8 nm (beam diameter of 0.63 mm) was used as an incident light being transmitted normal to the film surface, and an external ac electric field was applied across the composite film. The transmitted light intensity was measured with a photodiode without any polarizers under the modulation of an ac electric field. The rise response time, τ_R, for the light switching from a light scattering state to a transparent one (a random−homeotropic alignment change) was evaluated as the time required for a 10−90% transmittance change. The decay response time, τ_D, for the light switching from a transparent state to a light scattering one (a homeotropic−random alignment change) was also evaluated as the time required for a 90−10% transmittance change. The intensity of transmitted light as a function of the elapsed time was recorded with a digital storage oscilloscope to evaluate the memory effect for the composite systems. The distance between the cell and photodiode was 305 mm.

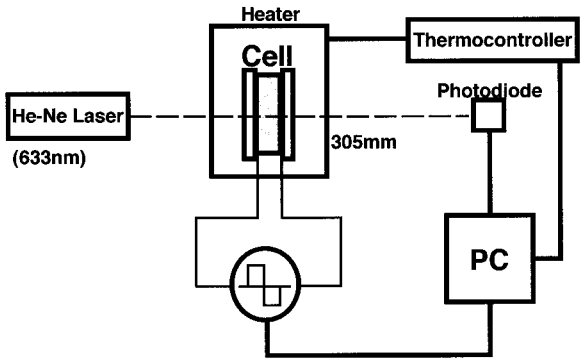

Figure 2. Schematic illustration of the measuring system for electro-optical properties of the composite system.

Results and Discussion

Characterization of Induced Smectic Composite Systems. Figure 3 shows the DSC curves and X-ray diffraction patterns of PS3EM(n = 24) and PS(3EM/DM)(n = 12). In order to obtain the reproducible DSC data, the third heating curves were used. The glass transition temperatures, T_g, of PS3EM(n = 24) and PS-(3EM/DM)(n = 12) were 288 and 262 K, respectively, as shown by the arrows in Figure 3. The DSC curve of PS3EM(n = 24) showed the small endothermic peak, T_{MI} at 344 K, as the mesophase−isotropic phase transition temperature. POM observation of PS3EM(n = 24) under crossed polarizers showed the schlieren texture, which is characteristic of the nematic phase over a temperature range above T_g and below T_{MI}. Also, the X-ray pattern of PS3EM(n = 24) at 293 K exhibited two diffuse rings corresponding to the spacings of 3.21 and 0.45 nm, respectively. The diffuse small-angle X-ray diffraction of PS3EM(n = 24) might be attributed to the

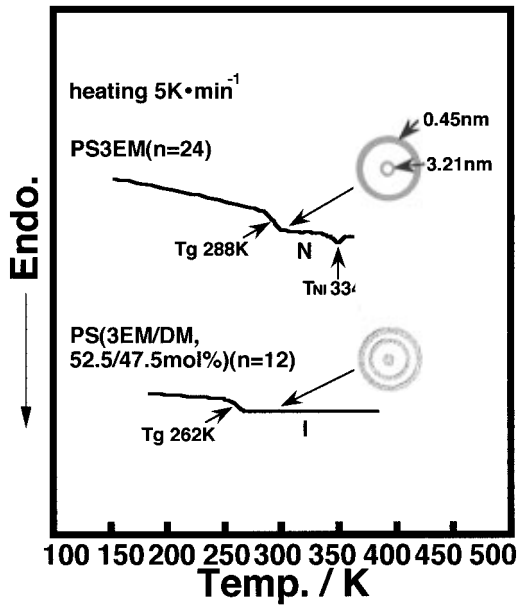

Figure 3. DSC curves and X-ray diffraction patterns of PS3EM(n = 24) and PS(3EM/DM)(n = 12).

length of mesogenic side chains along the long axis. The diffuse wide-angle X-ray diffraction of 0.45 nm spacing was associated with the average lateral approach distance of the side chain molecules. The X-ray diffraction patterns are also characteristic of the nematic phase. Therefore, the T_{MI} of PS3EM(n = 24) might be assigned as a nematic−isotropic phase transition temperature, T_{NI}. In the case of PS(3EM/DM)(n = 12), only a T_g shoulder was observed in the DSC curve. Also, no optical anisotropy was observed under POM. The X-ray pattern of PS(3EM/DM)(n = 12) showed three broad halo rings. The middle broad halo ring might correspond to the periodical packing distance of the main chains with the dimethylsiloxane groups in PS(3EM/DM)(n = 12). On the basis of the results mentioned above, PS(3EM/DM)(n = 12), which did not show any mesophases in the temperature range studied, is in an isotropic (amorphous) state. It is reasonable to consider that PS(3EM/DM)(n = 12) exhibited a lower T_g value and an amorphous state due to the lower molecular weight and the lower substituted fraction of mesogenic side chains, which induced a lower degree of anisotropic LC ordering.

The phase transition behaviors and the molecular dynamics of PS3EM(n = 24) and PS(3EM/DM)(n = 12) were confirmed by dielectric relaxation measurements. Two relaxation processes of PS3EM(n = 24) and PS(3EM/DM)(n = 12) were clearly observed as a function of temperature and frequency. Also, the dielectric relaxation measurement of poly[(methylsiloxane)-*co*-(dimethylsiloxane), 16.5/83.5 mol %](n = 29) (PHDS(n = 29)) was made to investigate the dielectric relaxation processes of a siloxane main chain. An apparent glass transition was confirmed at 146 K based on the DSC measurement. Figure 4 shows the Arrhenius plot for PS3EM(n = 24), PS(3EM/DM)(n = 12), and PHDS(n = 29). On the basis of the dielectric relaxation data for the oriented samples and the measurements of low molecular weight liquid crystals, it is concluded that the relaxation process at a higher temperature range (curves 1 and 2) is due to the α_a-relaxation process, which corresponds to the dynamic glass transition (micro-Brownian motion) of a main chain in LCP or pseudo LCcoP, although it may contain a contribution from the

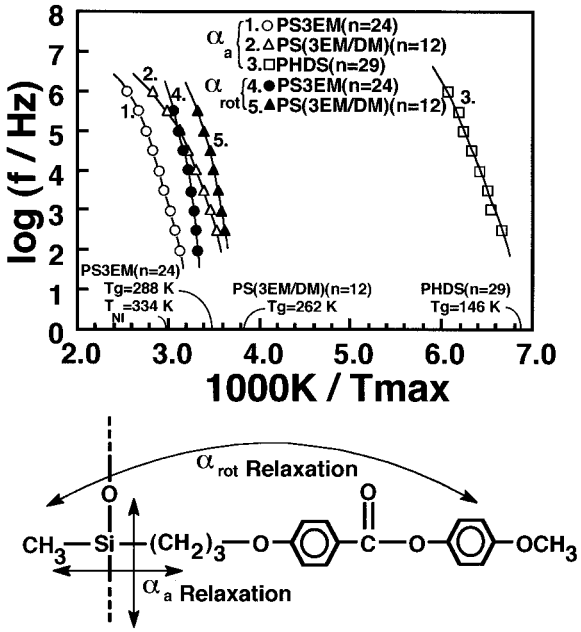

Figure 4. Arrhenius plot for relaxation frequencies of PS3EM-(n = 24), PS(3EM/DM)(n = 12), and PHDS(n = 29) as a function of reciprocal temperature and the scheme of the LCP structural unit and the relaxation movements that were observed in the dielectric relaxation measurements (indicated by arrows).

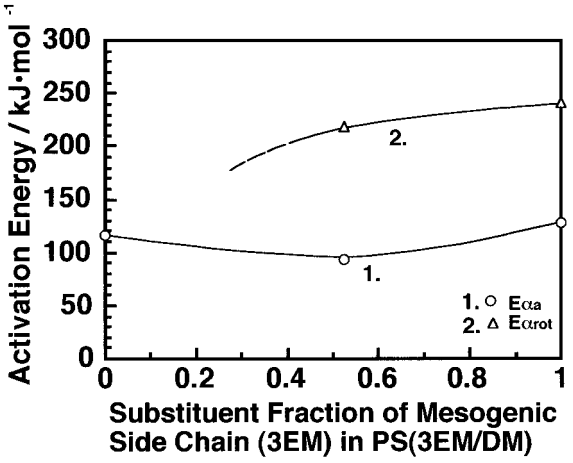

Figure 5. Magnitudes of activation energies for the α_a- and the α_{rot}-relaxation processes of PS(3EM/DM) vs the substituent fraction of mesogenic side chain (3EM) in PS(3EM/DM).

motions of the mesogenic groups. The relaxation process at the lower temperature range can be assigned to the α_{rot}-relaxation process, which is related to the rotation fluctuation of the mesogen side chain around its short axis, as shown in the lower part of Figure 4. Figure 5 shows the magnitudes of activation energies for the α_a- and the α_{rot}-relaxation processes of PS(3EM/DM) vs the substituent fraction of mesogenic side chain (3EM) in PS(3EM/DM). The magnitude of activation energy for the α_a-relaxation of PS(3EM/DM)(n = 12) was lower than that for PS3EM(n = 24). Furthermore, the α_a-relaxation frequency of PS(3EM/DM)(n = 12) was higher than that of PS3EM(n = 24), as shown in Figure 4. These results indicate that PS(3EM/DM)(n = 12) has a remarkably higher main chain mobility, which is influenced by the degree of polymerization and a plasticizing effect of the dimethylsiloxane groups on the siloxane backbone.

Figures 6 and 7 show the DSC curves and X-ray diffraction patterns of [PS3EM(n = 24)/E7] and [PS-

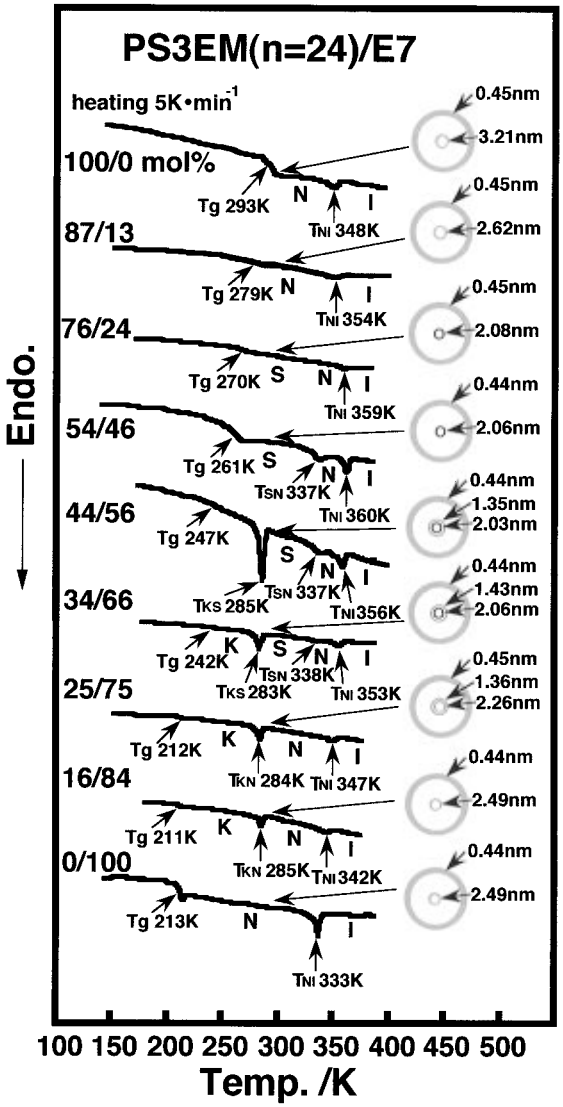

Figure 6. DSC curves and X-ray diffraction patterns of the [PS3EM(n = 24)/E7] composite system.

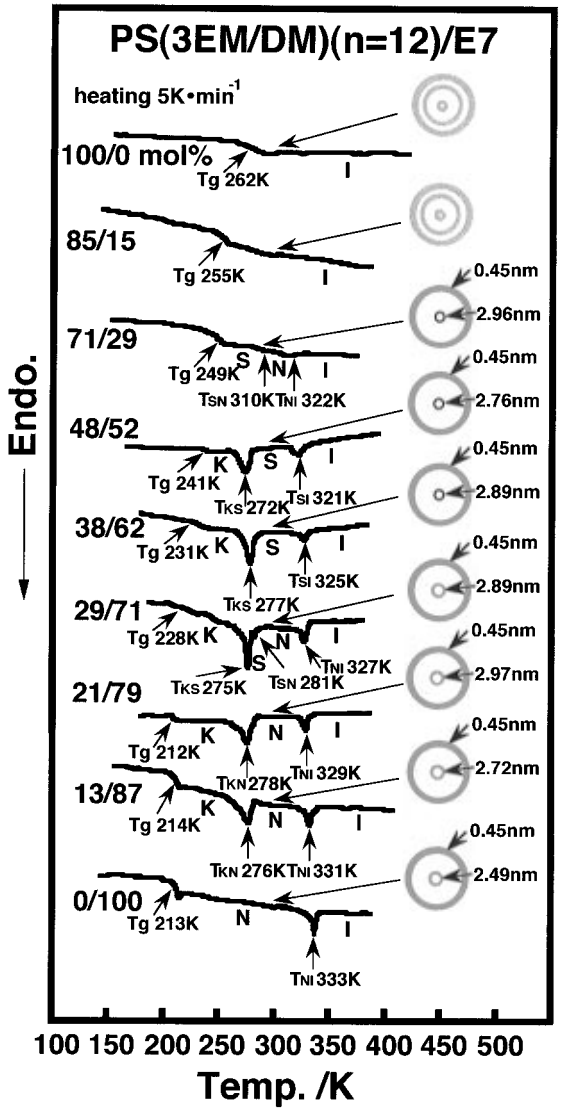

Figure 7. DSC curves and X-ray diffraction patterns of the [PS(3EM/DM)(n = 12)/E7] composite system.

(3EM/DM)(n = 12)/E7] composite systems. The T_g for the [PS3EM(n = 24)/E7] or [PS(3EM/DM)(n = 12)/E7] composite system decreased with an increase in the E7 fraction due to the plasticizing effect of E7. Since only one endothermic peak assigned to the mesophase−isotropic transition, T_{MI}, was measured, the composite systems might be in a homogeneously mixed mesomorphic phase (a molecularly dispersed state).[8,9] Therefore, it is reasonable to consider that E7 is miscible over a whole concentration range of PS3EM(n = 24) or PS(3EM/DM)(n = 12) in both isotropic and mesomorphic states. The assignments for isotropic, biphasic, and mesophase regions of the composite systems were also confirmed by POM observations. X-ray diffraction studies were also carried out in the mesophase state in order to investigate the aggregation state in the composites. The phase transition behaviors shown in Figures 6 and 7 were also confirmed on the basis of X-ray studies and POM observations. In a 34−76 mol % (40−80 wt %) range of PS3EM(n = 24) and a 38−71 mol % (50−80 wt %) range of PS(3EM/DM)(n = 12) for both binary composite systems, the sharp small angle X-ray scattering corresponding to an induced smectic layer structure was observed. Also, a fan-shape texture, characteristics of a smectic state, was observed under POM. These results indicate that [PS3EM(n = 24)/E7] and [PS(3EM/DM)(n = 12)/E7] composite systems showed a homogeneous induced smectic phase in these composite regions. In the case of PS3EM(n = 24) at fractions of 87 and 76 mol %, the composite systems show one endothermic peak corresponding to the nematic−isotropic phase transition temperature, T_{NI}, as shown in Figure 6. PS3EM(n = 24) at fraction of 76 mol % showed a smectic state near room temperature. The 54 mol % one shows two endothermic peaks relating to the smectic−nematic phase transition temperatures, T_{SN}, and T_{NI}, respectively. The 44 and 34 mol % ones show three endothermic peaks corresponding to the crystal−smectic phase transition temperature, T_{KS}, T_{SN}, and T_{NI}, respectively. The 25 and 16 mol % ones show two endothermic peaks in relation to the crystal−nematic phase transition temperature, T_{KN}, and T_{NI}, respectively. Since the composite system with the PS(3EM/DM)(n = 12) fraction of 85 mol % did not show any endothermic peaks in the temperature range studied here, the composite system was in an isotropic (amorphous) state, as mentioned above in the case of PS(3EM/DM)(n = 12), as shown in Figure 7. At 71 mol %, the composite system showed two endothermic peaks attributed to both T_{SN} and T_{NI}, respectively. The composite systems at 48 and 38 mol % show two endothermic peaks attributed to T_{KS} and the smectic−isotropic

phase transition temperature, T_{SI}, respectively. At fraction of 29 mol %, the composite systems shows three endothermic peaks attributed to T_{KS}, T_{SN}, and T_{NI}, respectively. The composite systems at fractions of 21 and 13 mol % showed two endothermic peaks attributed to T_{KN} and T_{NI}, respectively. Moreover, POM observation recognized that both the [PS3EM(n = 24)/E7] and the [PS(3EM/DM)(n = 12)/E7] composite systems exhibited the narrow biphasic mesophase−isotropic region of about 5 K wide below T_{NI} or T_{SI}, where the nematic or smectic and isotropic phases coexisted.

As shown in Figure 6, the [PS3EM(n = 24)/E7] composite systems with the PS3EM(n = 24) fraction of 44 and 34 mol % showed two sharp Debye rings in a small Bragg angle region, which might arise from the smectic layer structure. On the other hand, the [PS(3EM/DM)(n = 12)/E7] composite systems exhibited only one X-ray diffraction ring in a small angle region, as shown in Figure 7. Furthermore, in a nematic state the [PS3EM(n = 24)/E7] composite system with the PS3EM(n = 24) fraction of 25 mol % showed two diffuse Debye rings in a small Bragg angle region. The composite system with PS3EM(n = 24) at a fraction of 16 mol % showed one diffuse small angle X-ray diffraction ring. The inner diffuse ring was indicative of the short range order along the direction of the molecular long axes. Parts a and b of Figure 8 show the X-ray diffraction patterns for the induced smectic composite systems of [PS3EM(n = 24)/E7, 54/46 mol % (60/40 wt %)] (a) and [PS(3EM/DM)(n = 12)/E7, 48/52 mol % (60/40 wt %)] (b) at 295 K. It should be noted that in the [PS3EM(n = 24)/E7] composite systems, the inner ring is somewhat stronger and less diffuse than that in the [PS(3EM/DM)(n = 12)/E7] composite systems. Figure 9 shows the magnitude of layer spacing for both the [PS3EM(n = 24)/E7] and the [PS(3EM/DM)(n = 12)/E7] composite systems. The E7 molar fraction for the induced smectic phase was decided on the basis of the DSC studies mentioned in Figures 6 and 7. In the case of the induced smectic [PS3EM(n = 24)/E7] composite system, the magnitude of the layer spacing was almost equal to the length of a mesogenic side chain (3EM = 2.16 nm) in PS3EM(n = 24). This indicates that the mesogenic side chain region coexisting with LC molecules forms an induced smectic layer corresponding to one molecular length. For the [PS(3EM/DM)(n = 12)/E7] composite system, the magnitude of the layer spacing was somewhat longer than the length of a mesogenic side chain (3EM) in PS(3EM/DM)(n = 12), and much shorter than twice as long as the length of 3EM. From the results mentioned above, it seems reasonable to consider that since the rate of the volume occupied by the main chain including dimethylsiloxane groups in the [PS(3EM/DM)(n = 12)/E7] composite systems is higher than in the [PS3EM(n = 24)/E7] composite systems, the distance between the two siloxane main chains in an induced smectic layer spreads, and consequently, the smectic layer spacing becomes longer due to the deviation between the mesogenic side chains in pseudo LCcoP and LC molecules toward the direction of its long axis. In comparison with the case of the [PS3EM(n = 24)/E7] composite system, the induced smectic [PS(3EM/DM)(n = 12)/E7] composite system exhibited the broader half-width of the small-angle X-ray diffraction peak and also, the lower peak intensity of the maximum under the assumption of a Lorentzian line shape, as shown in Figure 8a,b. This indicates that the induced smectic [PS(3EM/DM)(n = 12)/E7] composite system might form more disordered smectic layers than the [PS3EM(n = 24)/E7] one.

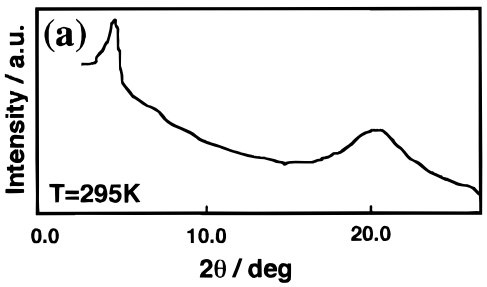

(a) [PS3EM(n=24)/E7, 54/46mol%(60/40wt%)]

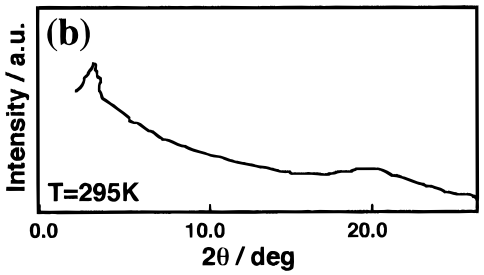

(b) [PS(3EM/DM)(n=12)/E7, 48/52mol%(60/40wt%)]

Figure 8. X-ray diffraction patterns for the induced smectic composite systems of [PS3EM(n = 24)/E7, 54/46 mol % (60/40 wt %)] (a) and [PS(3EM/DM)(n = 12)/E7, 48/52 mol % (60/40 wt %)] (b) at 295 K.

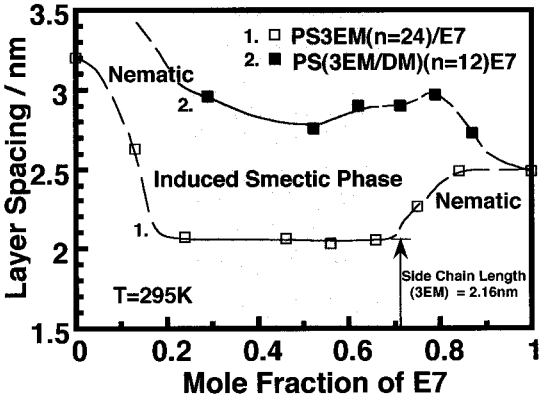

Figure 9. Magnitude of the layer spacing for both the [PS3EM(n = 24)/E7] and the [PS(3EM/DM)(n = 12)/E7] composite systems.

Parts a and b of Figure 10 show the phase diagrams of the [PS3EM(n = 24)/E7] (a) and the [PS(3EM/DM)(n = 12)/E7] (b) composite systems. These phase diagrams were obtained on the basis of the DSC and X-ray studies mentioned in Figures 6 and 7 and also POM observations. The phase diagrams are mainly divided into six regions, that is, (A) isotropic state, (B) biphasic (mesophase + isotropic) state, (C) mesophase (induced smectic or nematic) state, (D) crystalline (LCP or pseudo LCcoP + LCs) state, (E) crystalline (LCP or pseudo LCcoP + LCs) + mesophase (LCP or pseudo LCcoP + LCs) state, and (F) crystalline (LCP or pseudo LCcoP + LCs) + glassy mesophase (LCP or pseudo LCcoP + LCs) state. In the case of [PS3EM(n = 24)/E7], a homogeneous mesophase was formed over the whole mixing concentration of LCP. In the case of [PS(3EM/

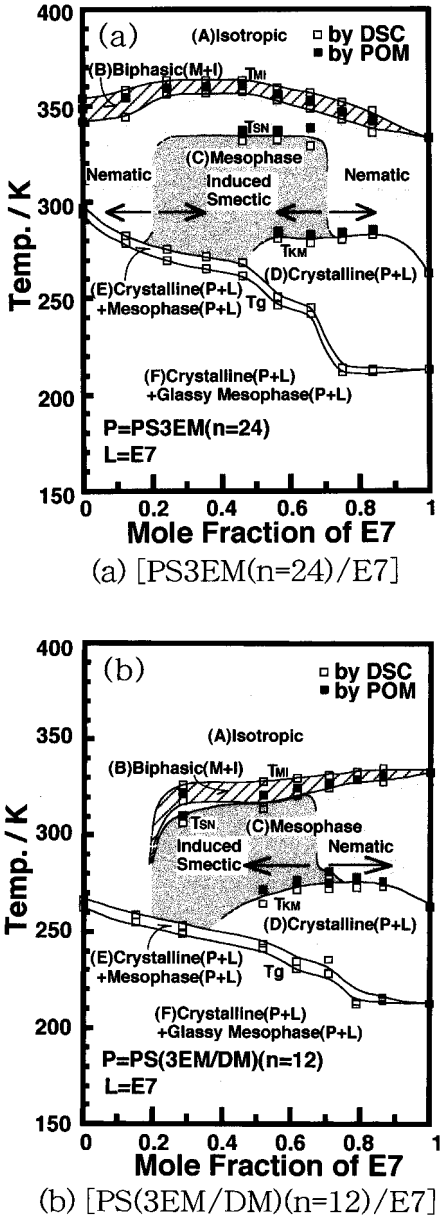

Figure 10. Phase diagrams of the [PS3EM(n = 24)/E7] (a) and the [PS(3EM/DM)(n = 12)/E7] (b) composite systems.

DM)(n = 12)/E7], a homogeneous mesophase was formed over the mixing range below 78 mol % (85 wt %) of pseudo LCcoP fraction. [PS3EM(n = 24)/E7] and [PS-(3EM/DM)(n = 12)/E7] composite systems were formed in the homogeneous induced smectic phase in the 29−81 mol % (35−85 wt %) range of PS3EM(n = 24) and in the 33−78 mol % (45−85 wt %) range of PS(3EM/DM)-(n = 12), respectively. In the series of these induced smectic binary composite systems composed of nematic LCP or pseudo LCcoP with weak polar methoxy terminal groups and nematic LCs with each strong polar cyano terminal group, a definite fraction range of approximately 30−80 mol % of LCP or pseudo LCcoP is necessary to construct the induced smectic phase, in analogy with the binary mixtures of nematic LCs. The homogeneous induced smectic phase played an important role in realizing an excellent memory effect due to its remarkable high viscosity in comparison with that in a nematic state.[16,17] Although PS(3EM/DM)(n = 12) did not show any mesophases states in the temperature range studied here, as mentioned in Figures 7 and 10b,

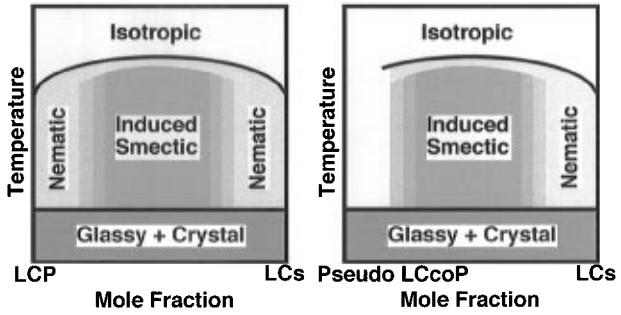

(a) Induced Smectic (Nematic LCP / Nematic LC) Composite System

(b) Induced Smectic (Pseudo LCcoP / Nematic LC) Composite System

Figure 11. Schematic comparison of phase diagrams of the induced smectic (nematic LCP/nematic LCs) composite system (a) and induced smectic (pseudo LCcoP/nematic LCs) composite system (b).

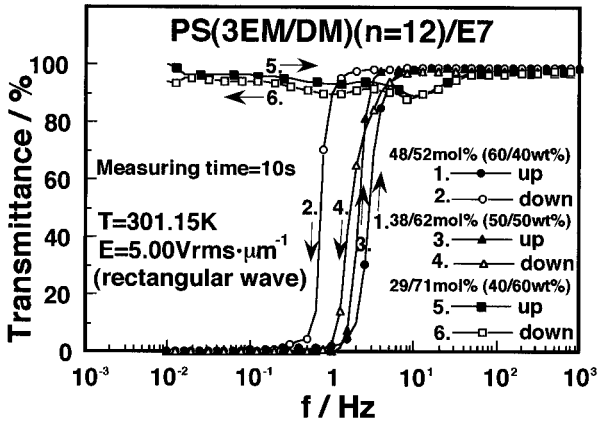

Figure 12. Frequency dependence of the transmittance for the [PS(3EM/DM)(n = 12)/E7] composite systems.

the [PS(3EM/DM)(n = 12)/E7] composite system formed a homogeneous induced smectic phase in the 33−78 mol % range of PS(3EM/DM)(n = 12). This indicates that though the pseudo LCcoP is amorphous, this has the possibility of forming an induced smectic phase when E7 is mixed with amorphous LCcoP as the binary composite system. The temperature range of an induced smectic state for [PS(3EM/DM)(n = 12)/E7] was lower than that for the [PS3EM(n = 24)/E7] one. Thus, the induced smectic (pseudo LCcoP/nematic LCs) composite system might be expected as the novel type of LC display with a bistable memory effect and with a short response time. We can represent the composite system in a simple diagram in comparison with the induced smectic (nematic LCP/nematic LCs) composite system, as shown in Figure 11.

Electro-optical Properties of the Induced Smectic Composite Systems. In the case of the induced smectic (nematic LCP/nematic LCs) composite systems studied here, a polar balance between nonpolar terminal groups of the LCP and polar terminal groups of LCs can be changed by means of varying the mixing concentration in order to control the strength of an induced smectic layer and, also, to improve the electro-optical switching speed. [PS(3EM/DM)(n = 12)/E7] could be used as the induced smectic state over a wide range of 33−78 mol % (45−85 wt %) of PS(3EM/DM)(n = 12) at room temperature, as shown in Figure 10b. Figure 12 shows the frequency dependence of the transmittance for [PS(3EM/DM)(n = 12)/E7] with the different component fractions under an electric field of E = 5.00 Vrms·μm^{-1} at 301 K. A reversible and bistable light

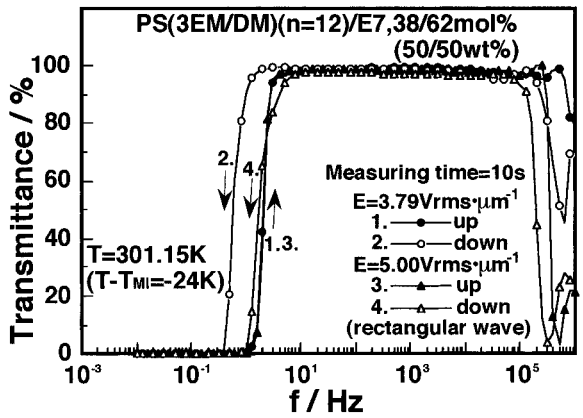

Figure 13. Frequency dependence of the transmittance for the [PS(3EM/DM)(n = 12)/E7, 38/62 mol % (50/50 wt %)] composite system.

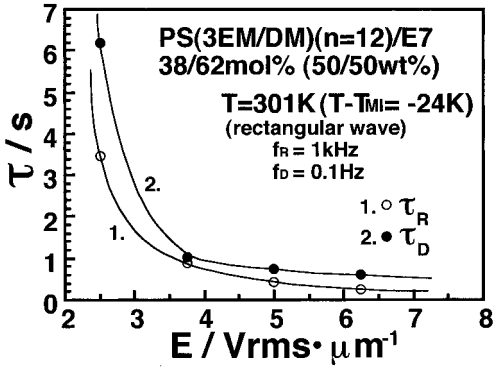

Figure 14. Relationship between rise and decay response times (τ_R, τ_D) and the applied electric field for the [PS(3EM/DM)(n = 12)/E7, 38/62 mol % (50/50 wt %)] composite system.

switching was recognized for [PS(3EM/DM)(n = 12)/E7, 48/52 mol % (60/40 wt %)] and [PS(3EM/DM)(n = 12)/E7, 38/62 mol % (50/50 wt %)] in an induced smectic state at room temperature. Each composite system exhibited a highly transparent state upon application of a high-frequency ac electric field (1 kHz) due to the electric field effect based on the dielectric anisotropy of the LC molecules and the side chain part of the pseudo LCcoP and also, a remarkable light scattering state upon the application of a low-frequency ac electric field (0.1 Hz) owing to the electric current effect based on the electrohydrodynamic motion of the LCcoP main chains. The transparent and turbid states were stable, even though ac electric fields were turned off. [PS(3EM/DM)(n = 12)/E7, 48/52 mol % (60/40 wt %)] exhibited some hysteresis in the increasing and decreasing processes of the electric field frequency. This may be due to the high aggregation stability obtained by the homeotropic alignment composed of smectic domains. For nematic [PS(3EM/DM)(n = 12)/E7, 29/71 mol % (40/60 wt %)] a light scattering state was not observed, even under a low-frequency ac electric field (0.1 Hz). The composite system also showed a low contrast and did not show a memory effect due to a homogeneous nematic state. These results indicate that since the change in the mixing concentration of pseudo LCcoP and LCs for the binary composite system directly corresponds to the change in the polar balance between terminal groups of the binary components, the viscosity of the binary composite system and the mechanical strength of the smectic layer depend strongly on the components fraction.

Figure 13 shows the frequency dependence of the transmittance for [PS(3EM/DM)(n = 12)/E7, 38/62 mol % (50/50 wt %)] under E = 3.79 Vrms·μm^{-1} and E = 5.00 Vrms·μm^{-1} at 301 K. In the case of E = 3.79 Vrms·μm^{-1}, the binary composite system exhibited some hysteresis in the increasing and decreasing processes of the electric field frequency. This may be due to the aggregation stability obtained by the homeotropic alignment composed of smectic domains. At E = 5.00 Vrms·μm^{-1}, the system did not show hysteresis. It is worth noting that though the binary composite system showed a highly transparent state in the frequency range from 10 Hz to 100 kHz, the system changed to a light scattering state in the higher frequency region, similarly to the low-frequency region. Since the dielectric anisotropy of both LC molecules and the side chain part of the pseudo LCcoP was reversed from positive to negative in the higher frequency region in analogy with low molecular weight nematic LCs,[20,21] it is reasonable that a light scattering state was formed in this ac frequency region. When the reversible light switching was repeated many times under the application of ac electric fields with low (dc or ~0.1 Hz) and high frequencies (~kHz), damage of the cell for the binary composite system was possible because of the electric current effect accompanying an ionic current upon the application of a low-frequency electric field. Therefore, the bistable and reversible light switching driven by ac electric fields with high (~kHz) and higher frequencies (~100 kHz) should be useful to construct the binary composite systems having an excellent durability, because the ionic current should not be induced in the higher frequency region above ~kHz.

Figure 14 shows the relationship between rise and decay response times (τ_R, τ_D) and the magnitude of the applied electric field for [PS(3EM/DM)(n = 12)/E7, 38/62 mol % (50/50 wt %)] upon the application of low (0.1 Hz) and high (1 kHz) driving frequency ac electric fields. A reversible and bistable electro-optical switching with quite shorter response times (~100 ms) at room temperature was realized for [PS(3EM/DM)(n = 12)/E7, 38/62 mol %] under the application of an ac electric field above 4 Vrms·μm^{-1}, as shown in Figure 14. Also, in the case of the application of high (1 kHz) and higher (300 kHz) driving frequency ac electric fields, the binary composite system showed a reversible and bistable electro-optical switching with much the same response times (~100 ms) at room temperature. The turbid (light scattering) and the transparent states for the composite system were stable for a long period (more than 3 years) at room temperature. On the other hand, [PS3EM(n = 24)/E7] did not exhibit a fast bistable electro-optical switching, but the response times ranged above several seconds under an appropriate electric field strength at room temperature. We conclude from the results mentioned above that the introduction of pseudo LCcoP into the induced smectic composite systems is strikingly effective in reducing the electro-optical switching times with a stable memory effect at room temperature.

Conclusions

A pseudo liquid crystalline copolymer (pseudo LCcoP) with weak polar methoxy terminal groups in the side chains was used in order to improve the bistable light switching speed of the induced smectic binary composite system at room temperature. The pseudo LCcoP with substituted mesogenic side chains of 52.5 mol % did not exhibit any mesophase characteristics. However, the binary composite showed an induced smectic phase over

a wide range of both mixing concentration (33−78 mol % of LCcoP) and temperature (250−320 K). A novel type of phase diagram for an induced smectic binary composite system, the induced smectic (pseudo LCcoP with weak polar methoxy terminal groups/nematic LCs with each strong polar cyano terminal group) composite system, was developed. A reversible and bistable electro-optical switching with a short response time (∼100 ms) at room temperature was realized for the binary composite system in the induced smectic state. Also, the binary composite system showed a reversible and bistable electro-optical switching based on the sign reversal of the dielectric anisotropy upon the application of ac electric fields with high (∼kHz) and higher (∼100 kHz) driving frequencies. Introduction of pseudo LCcoP with a small substituent fraction of mesogenic side chains into the induced smectic binary composite system is extremely effective in order to improve the switching speed of the binary composite system.

References and Notes

(1) McArdle, C. B., Ed. In *Side Chain Liquid Crystal Polymers*; Blackie and Chapman and Hall, Inc.: Glasgow, London, New York, 1989.
(2) Shibaev, V. P.; Kostromin, S. G.; Plate, N. A.; Ivanov, S. A.; Vetrov, V. Yu.; Yakoviev, I. A. *Polym. Commun.* **1983**, *24*, 364.
(3) Simon, R.; Cole, H. J. *Mol. Cryst. Liq. Cryst.* **1984**, *102*, 43. Cole, H. J.; Simon, R. *Polymer* **1985**, *26*, 1801.
(4) Ueno, T.; Nakamura, T.; Tani, C. *Proc. Jpn Display* **1986**, 190.
(5) McArdle, C.; Clark, M.; Haws, C.; Wiltshire, M.; Parker, A.; Nestor, G.; Gray, G.; Lacey, D.; Toyne, K. *Liq. Cryst.* **1987**, *2*, 573.
(6) Hopwood, A. I.; Coles, H. J. *Polymer* **1985**, *26*, 1312.
(7) Sefton, M. S.; Coles, H. J. *Polymer* **1985**, *26*, 1319.
(8) Kajiyama, T.; Kikuchi, H.; Miyamoto, A.; Moritomi, S.; Hwang, J. C. *Chem. Lett.* **1989**, *1989*, 817−820.
(9) Kikuchi, H.; Moritomi, S.; Hwang, J. C.; Kajiyama, T. *Polym. Adv. Technol.* **1990**, *1*, 297−300.
(10) Kajiyama, T.; Kikuchi, H.; Hwang, J. C.; Miyamoto, A.; Moritomi, S.; Morimura, Y. *Prog. Pacific Polym. Sci.* **1991**, 343−354.
(11) Kajiyama, T.; Yamane, H.; Kikuchi, H.; Hwang, J. C. In *Liquid-Crystalline Polymer Systems Technological Advances*; Isayev, A. I., Kyu, T., Cheng, S. Z. D., Eds.; ACS Symposium Series No. 632; American Chemical Society: Washington, DC, 1996; Chapter 12, p 190.
(12) Griffin, A. C.; Johnson, J. F. *J. Am. Chem. Soc.* **1977**, *99*, 4859.
(13) Engelen, B.; Heppke, G.; Hopf, R.; Schnider, F. *Ann. Phys.* **1978**, *3*, 403.
(14) Domon, M.; Billard, J. *J. Phys., Paris* **1979**, *40*, C3−413.
(15) Schneider, F.; Sharna, N. K. *Z. Naturforsch.* **1981**, *36*, 62.
(16) Kajiyama, T.; Kikuchi, H.; Miyamoto, A.; Moritomi, S.; Hwang, J. C. *Mater. Res. Soc. Symp. Proc.* **1990**, *171*, 305.
(17) Hwang, J. C.; Kikuchi, H.; Kajiyama, T. *Polymer* **1992**, *33*, 1822−1825.
(18) Yamane, H.; Kikuchi, H.; Kajiyama, T. *Polym. Prepr. Jpn.* **1992**, *41*, 3719−3721.
(19) Finkelmann, H.; Kock, H.; Rehage, G. *Makromol. Chem., Rapid. Commun.* **1981**, *2*, 317.
(20) Meier, G.; Saupe, A. *Proceedings of the First International Conference on Liquid Crystals*; Gordon and Breach: New York, 1965; p 195.
(21) Bucher, H. K.; Klingbiel, R. T.; VanMeter, J. P. *Appl. Phys. Lett.* **1974**, *25*, 186.

MA961754U